Available online at www.sciencedirect.com
ScienceDirect
Journal of Power Sources 179 (2008) 361–366
JOURNAL OF POWER SOURCES
www.elsevier.com/locate/jpowsour

Short communication

Electrochemical synthesis of birnessite-type layered manganese oxides for rechargeable lithium batteries

Masaharu Nakayama [a], Taku Kanaya [a], Jong-Won Lee [b], Branko N. Popov [b,*]

[a] *Department of Applied Chemistry, Yamaguchi University, Ube 755–8611, Japan*
[b] *Center for Electrochemical Engineering, Department of Chemical Engineering, University of South Carolina, Columbia, SC 29208, USA*

Received 6 December 2007; received in revised form 13 December 2007; accepted 14 December 2007
Available online 31 December 2007

Abstract

Layered manganese dioxide (MnO_2) films intercalated with Li^+, Na^+ or Mg^{2+} ions were synthesized by a one-step electrochemical method. The electrodeposition was potentiostatically performed by applying an anodic potential of 1.0 V vs. Ag/AgCl in an aqueous $MnSO_4$ solution containing a perchlorate salt of the cation. The electrodeposited oxide films have a birnessite-type layered structure with alkali cations and water molecules between manganese oxide layers. The galvanostatic charge–discharge experiments performed in 1 M $LiPF_6$-DME/PC solution indicated that the Mg^{2+}-intercalated MnO_2 electrode exhibits an initial discharge capacity as large as 140 mAh g^{-1} and it shows a better capacity retention during cycling as compared with the Li^+- or Na^+-intercalated MnO_2 electrode.

Keywords: Birnessite; Electrodeposition; Layered structure; Manganese oxide; Lithium battery

1. Introduction

Transition metal oxides can intercalate and deintercalate lithium ions at high potentials with respect to a carbon anode. $LiCoO_2$ has become the cathode of choice in commercial lithium-ion batteries. It has a well-ordered layered crystal structure with an $R\bar{3}m$ symmetry that allows reversible lithium intercalation and deintercalation. However, high cost and toxicity of cobalt have been stimulating researches to develop alternative cathode materials based on manganese oxides.

A layered lithium manganese oxide (Li_xMnO_2) with an $R\bar{3}m$ rhombohedral structure has attracted much attention due to its large theoretical capacity as well as economic and environmental merits [1,2]. Many attempts have been made to prepare layered Li_xMnO_2 by 'soft' chemistry routes such as ion-exchange methods [3–5]. The synthesized materials were found to show a monoclinic structure ($C2/m$) due to a cooperative distortion of the MnO_6 octahedra, rather than a perfect rhombohedral structure [2–5]. Also, it has been reported that monoclinic Li_xMnO_2 is easily transformed to the thermodynamically stable spinel-phase within a few charge–discharge cycles, leading to a significant capacity loss [2,5].

A birnessite-type manganese oxide has a two-dimensional layered structure that consists of edge-sharing MnO_6 octahedra with water molecules in the interlayer space [6]. Fig. 1 presents schematically the crystal structure of a birnessite-type manganese oxide. The manganese oxide layer is negatively charged due to the presence of Mn^{3+} ions, and thus alkali metal cations or organoammonium ions are also intercalated in the interlayer region depending on the precursors used. Owing to its relatively open structure, birnessite-type MnO_2 is believed to provide more favorable pathways for lithium intercalation and deintercalation as compared with monoclinic oxides.

Various methods have been developed to synthesize birnessite-type MnO_2–including sol–gel reactions [6–8], calcinations [9], and hydrothermal decomposition of a $LiMnO_4$, $NaMnO_4$ or $KMnO_4$ precursor [10–13]. Recently, a new electrochemical method was developed at Yamaguchi University to synthesize birnessite-type layered MnO_2 intercalated with organic molecules such as alkylammonium ions [14,15] and polycations [16]. The electrodeposition process involves a

* Corresponding author. Tel.: +1 803 777 7314; fax: +1 803 777 8265.
E-mail address: popov@engr.sc.edu (B.N. Popov).

0378-7753/$ – see front matter © 2007 Elsevier B.V. All rights reserved.
doi:10.1016/j.jpowsour.2007.12.075

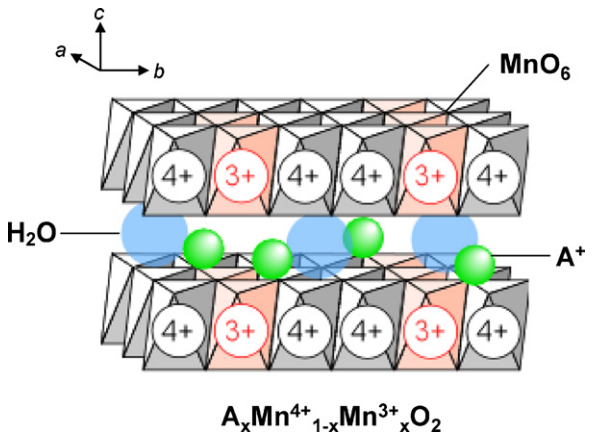

Fig. 1. Schematic diagram of a birnessite-type layered manganese oxide incorporated with alkali cations.

potentiostatic oxidation of aqueous Mn^{2+} ions in the presence of a small amount of organic molecules. Effect of several parameters such as the type of organic molecules, bath composition, and applied potential on the structure of MnO_2 has been studied. The formation of layered MnO_2 was achieved only when the manganese concentration in the electrolyte bath was lower than 10 mM, and the interlayer distance increased with increasing alkyl chain length, confirming the presence of organic molecules between manganese oxide layers.

Electrodeposition technique is used in this paper to synthesize a birnessite-type layered MnO_2 intercalated with alkali metal cations (Li^+, Na^+ or Mg^{2+}). The charge–discharge characteristics of birnessite-type layered MnO_2 as cathode material for rechargeable lithium batteries were evaluated in 1 M $LiPF_6$-DME/PC solution.

2. Experimental

2.1. Electrochemical synthesis of manganese oxides

All chemicals were reagent grade (Aldrich) and were used without further purification. All solutions were prepared with distilled water and deaerated by bubbling with purified argon gas for over 20 min prior to use. Electrodeposition was performed using a conventional three-electrode cell (T-cell). A platinum gauze and a Ag/AgCl electrode (in saturated KCl) were used as the counter and reference electrodes, respectively. A gold-sputtered stainless steel substrate was used as the working electrode. The deposition bath used was 2 mM $MnSO_4$ solution mixed with 50 mM $LiClO_4$, 50 mM $NaClO_4$, or 25 mM $Mg(ClO_4)_2$. An EG&G PAR model 273A potentiostat/galvanostat was used for electrodeposition. A constant potential of 1.0 V vs. Ag/AgCl was applied to the working electrode, and then the current (or the electric charge delivered) was monitored as a function of time.

The weight of the electrodeposited oxide film was determined by using electrochemical quartz crystal microbalance (EQCM). The experiments were carried out using a QCA917 quartz crystal analyzer (Seiko EG&G). An AT-cut 9 MHz Pt-plated quartz crystal (Seiko EG&G model OA-A9M-PT) with an area of 0.16 cm^2 was used as the working electrode. The electrodeposited oxide film was rinsed thoroughly with deionized water, and then dried under vacuum at 80 °C for over 3 h prior to materials characterizations and electrochemical measurements.

2.2. Materials characterizations

X-ray diffraction (XRD) data were recorded using a Shimadzu XD-D1 diffractometer with Cu Kα radiation ($\lambda = 0.15405$ nm). The data were collected in the 2θ range from 5° to 50° with a scan rate of 1° min^{-1}. The beam voltage was 30 kV, and the beam current was 30 mA. Field emission-scanning electron microscopy (FE-SEM) images were obtained at an accelerating voltage of 20 kV with a Hitachi S-4700Y scanning electron microscope.

2.3. Electrochemical experiments

Galvanostatic charge–discharge experiments were performed with an EG&G PAR model 273A potentiostat/galvanostat. A three-electrode cell was employed for the electrochemical measurements. Both the counter and reference electrodes were constructed from lithium foil (electrochemical grade, FMC Corporation). The electrolyte used was 1 M $LiPF_6$ solution in DME and PC (50:50, vol.%, Ferro Corporation). Galvanostatic charge–discharge curves were measured with a current density of 10 μA cm^{-2} in the potential range between 2.0 and 4.2 V vs. Li/Li^+.

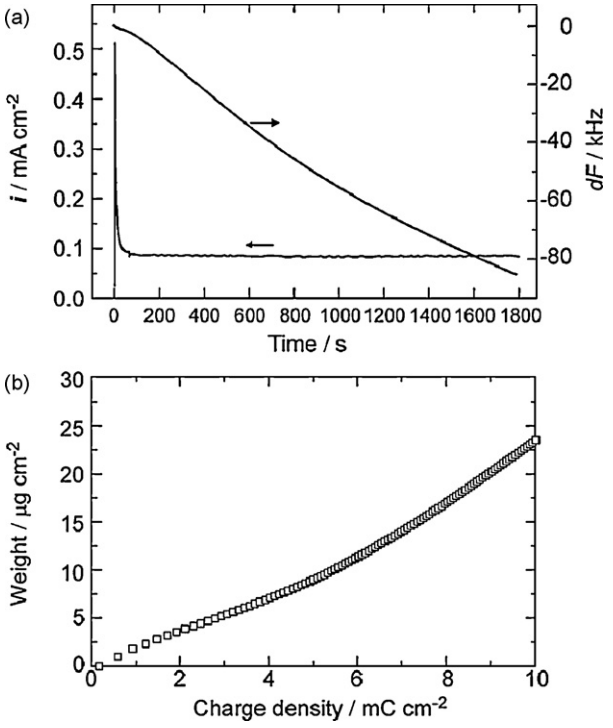

Fig. 2. (a) Typical current and frequency profiles measured simultaneously on a quartz crystal during electrodeposition in $LiClO_4$-containing $MnSO_4$ solution, and (b) plot of weight versus charge density reproduced from (a).

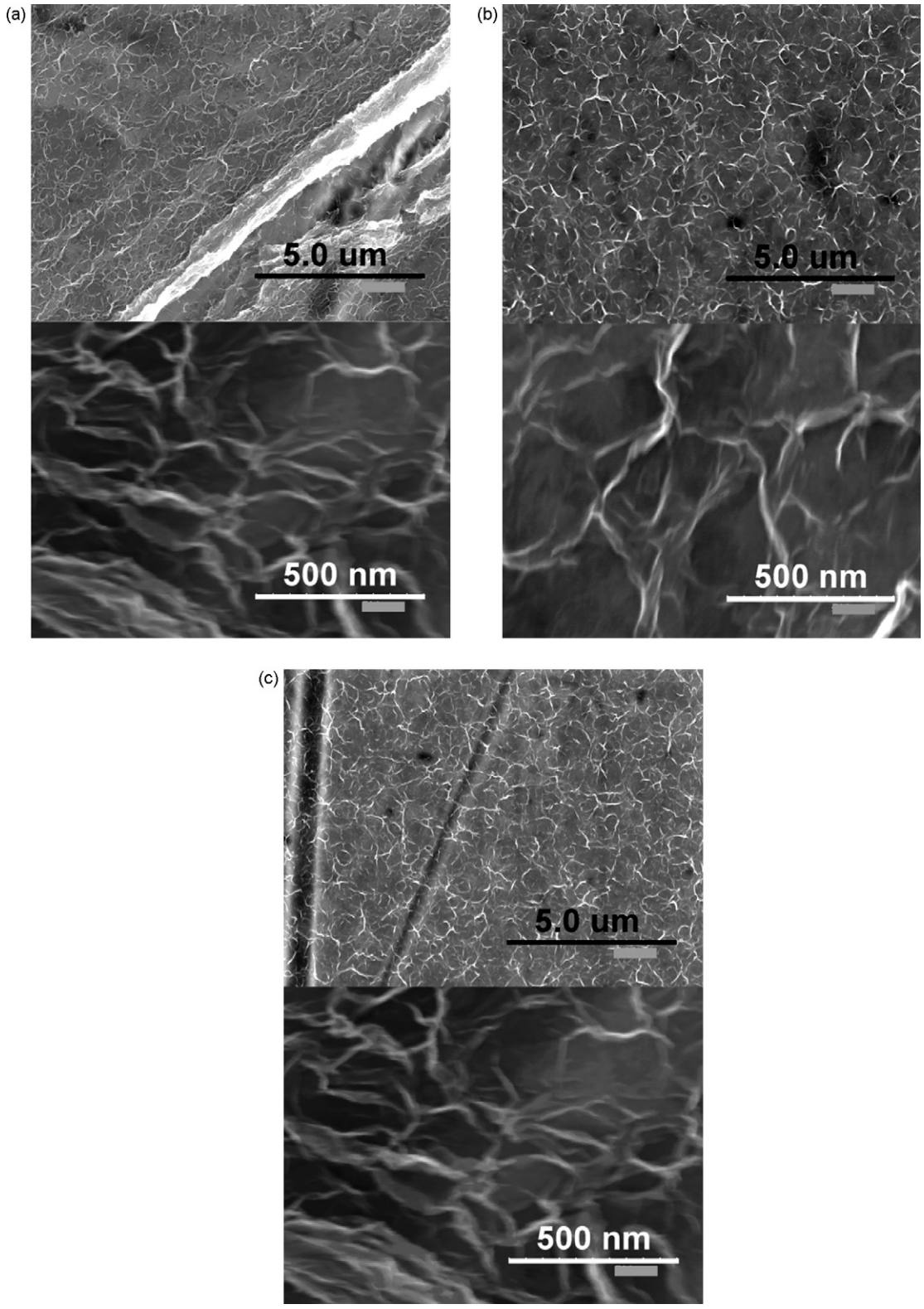

Fig. 3. FE-SEM images of the manganese oxide films electrodeposited from $MnSO_4$ solution in the presence of (a) $LiClO_4$, (b) $NaClO_4$, and (c) $Mg(ClO_4)_2$.

3. Results and discussion

3.1. Electrochemical synthesis and characterizations of manganese oxide electrodes

Fig. 2(a) shows typical current and frequency profiles measured simultaneously on a quartz crystal during electrodeposition in a $LiClO_4$-containing $MnSO_4$ solution. The current transient shows a rapid current decay with time, followed by a current plateau. During the anodic deposition reaction, the electrons produced by oxidation of Mn^{2+} ions should be transferred from the deposited film to the underlying substrate. The appearance of the constant anodic current in the current transient suggests that the deposited film is conductive enough not to block electron transfer to the substrate. As shown in Fig. 2(a), the frequency decreases linearly with time, indicating an increase in the electrode mass due to electrodeposition.

Fig. 2(b) presents the plot of weight versus charge density reproduced from Fig. 2(a). The charge density was calculated by integrating the measured current with respect to time. The weight change per unit area (Δm) was calculated from the frequency change (Δf) of the quartz crystal electrode using the well-known Sauerbrey equation [17]:

$$\Delta f = -\frac{2f_o^2}{\sqrt{\mu\rho}}\Delta m = -C\,\Delta m \quad (1)$$

where f_o is the resonance frequency, μ is the shear modulus, and ρ is the density of the quartz crystal. In this study, the integral sensitivity constant (C) was determined to be $1.97 \times 10^8\ cm^2\ s^{-1}\ g^{-1}$ from galvanostatic silver deposition experiments. The weight versus charge density curve yielded a slope of $1.58\ g\ C^{-1}$ that translates to $152.4\ g\ mol^{-1}$ of electrons. This value is larger than that ($86.94\ g\ mol^{-1}$ of electrons) calculated based on the following electrochemical reaction for manganese oxide formation:

$$Mn^{2+} + 2H_2O \rightarrow 2MnO_2 + 4H^+ + 2e^- \quad (2)$$

The result indicated incorporation of Li^+ ions and water molecules into the manganese oxide during electrodeposition. In a birnessite-type manganese oxide, the oxide layer is negatively charged due to the presence of Mn^{3+} ions which allows alkali metal cations to intercalate into the interlayer space during electrodeposition. Thus, the formation of manganese during electrodeposition can be expressed as:

$$Mn^{2+} + (2+n)H_2O + xA^{c+} \rightarrow A_{x/c}Mn^{3+}{}_xMn^{4+}{}_{1-x}O_2 \cdot nH_2O + 4H^+ + (2-x)e^- \quad (n \approx 1) \quad (3)$$

where A is the alkali cation and c is 1 for Li^+ and Na^+, or 2 for Mg^{2+}. The previous study [15] indicated that the amount of alkali cations depends on the bath composition and the applied potential. From the X-ray photoelectron spectroscopy, x was estimated to be approximately 0.35 in this study. The amount of divalent magnesium ions incorporated into the structure is half that of monovalent lithium or sodium ions.

Fig. 3(a–c) shows the FE-SEM images of the surfaces of the manganese oxide films electrodeposited from a $MnSO_4$ solution in the presence of $LiClO_4$, $NaClO_4$ or $Mg(ClO_4)_2$, respectively. It is seen that all the oxide films have uniform surfaces with a sheet-like morphology (see higher magnification images).

Fig. 4 demonstrates the XRD patterns of the manganese oxide films incorporated with Li^+, Na^+, or Mg^{2+} ions. As a reference, the powder XRD pattern of K-type birnessite synthesized through a chemical route is also presented in this figure. The XRD patterns of the electrodeposited oxide films were in good agreement with the pattern of the reference sample. As indicated in Fig. 3, the diffraction peaks at $2\theta = 12.3^\circ$ and 24.7° are assigned to (0 0 1) and (0 0 2) planes of a birnessite-type layered structure, respectively. The d_{001} value was calculated to be approximately 0.72 nm for all the oxide films, which confirms the presence of water molecules in the interlayer space.

3.2. Charge–discharge characteristics of the electrodeposited manganese oxide electrodes

Fig. 5(a) shows the initial discharge curves of $Li_{0.35}MnO_2{\cdot}H_2O$, which were measured in 1 M $LiPF_6$-DME/PC solution using a current density of $10\ \mu A\ cm^{-2}$. The electrodeposition was carried out for 30, 60 and 90 min. The potential decreases continuously with progressing discharge without any potential plateau regions, which indicates that a single phase is maintained over the whole composition range. As expected, the discharge capacity determined at 2.0 V vs. Li/Li^+ increased linearly from 5 to $11.6\ \mu Ah\ cm^{-2}$ with deposi-

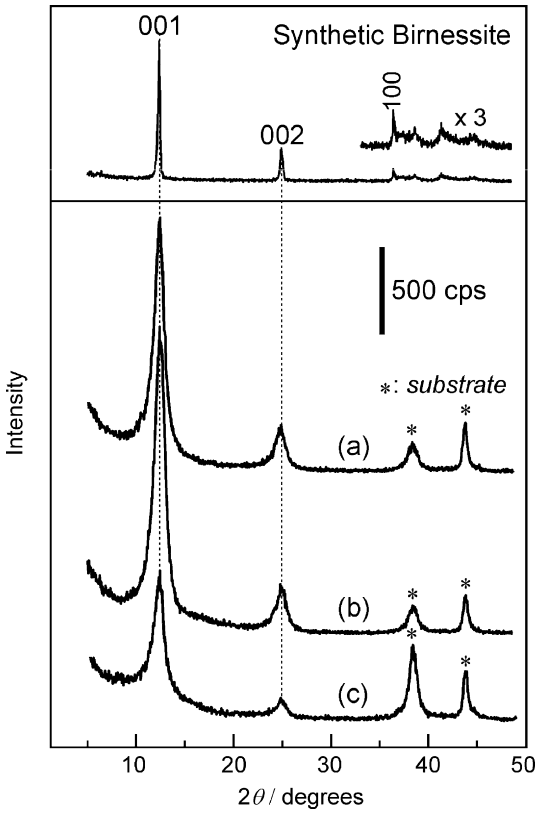

Fig. 4. XRD patterns of the manganese oxide films electrodeposited from $MnSO_4$ solution in the presence of (a) $LiClO_4$, (b) $NaClO_4$, and (c) $Mg(ClO_4)_2$.

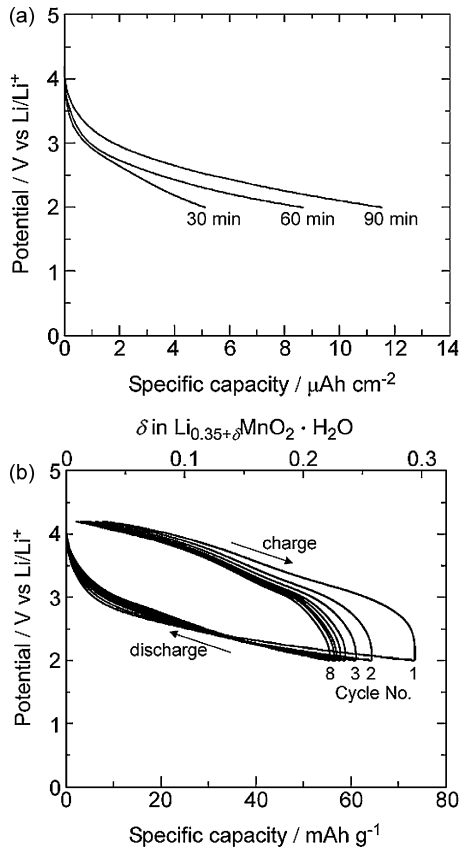

Fig. 5. (a) Initial discharge curves of $Li_{0.35}MnO_2{\cdot}H_2O$ electrodeposited for different times, and (b) charge–discharge curves of the electrode electrodeposited for 60 min. The data were obtained in 1 M $LiPF_6$-DME/PC solution using a current density of 10 μA cm^{-2}.

tion time. This confirms that the entire volume of the oxide film is electrochemically active for lithium intercalation. Fig. 5(b) presents the charge–discharge curves of $Li_{0.35}MnO_2{\cdot}H_2O$ electrodeposited for 60 min. The initial gravimetric discharge capacity was determined to be ca. 73 mAh g^{-1}, but the capacity decreased rapidly to 56 mAh g^{-1} after 8 cycles.

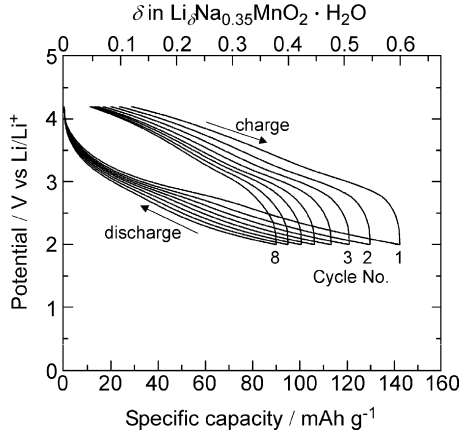

Fig. 6. Galvanostatic charge–discharge curves of the $Na_{0.35}MnO_2{\cdot}H_2O$ electrode measured in 1 M $LiPF_6$-DME/PC solution using a current density of 10 μA cm^{-2}.

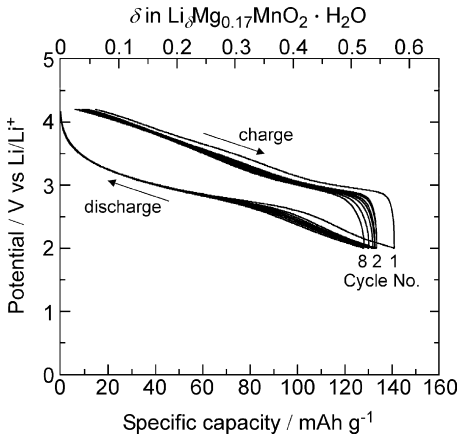

Fig. 7. Galvanostatic charge–discharge curves of the $Mg_{0.17}MnO_2{\cdot}H_2O$ electrode measured in 1 M $LiPF_6$-DME/PC solution using a current density of 10 μA cm^{-2}.

The galvanostatic charge–discharge curves of $Na_{0.35}MnO_2{\cdot}H_2O$ are shown in Fig. 6. The $Na_{0.35}MnO_2{\cdot}H_2O$ electrode exhibits a higher initial capacity of 140 mAh g^{-1} than $Li_{0.35}MnO_2{\cdot}H_2O$. However, the Na^+-intercalated MnO_2 electrode shows a drastic capacity decay with cycling. Fig. 7 depicts the charge–discharge curves of $Mg_{0.17}MnO_2{\cdot}H_2O$ electrode. The Mg^{2+}-intercalated MnO_2 electrode shows the same initial discharge capacity of 140 mAh g^{-1} as $Na_{0.35}MnO_2{\cdot}H_2O$. However, as shown in Fig. 7, $Mg_{0.17}MnO_2{\cdot}H_2O$ exhibits much better capacity retention during cycling in comparison with $Na_{0.35}MnO_2{\cdot}H_2O$.

Chen and Whittingham [12] proposed that the degradation of capacity on cycling of birnessite-type Li_xMnO_2 results mainly from deintercalation of lithium ions from the interlayer space during cell charge followed by migration of manganese from the MnO_2 layers to the interlayer region. In order to maintain high capacity on cycling, therefore, alkaline cations should be immobilized so that they can prevent the collapse of the layered structure due to manganese migration into the interlayer space and to allow the oxides to be stabilized in a hexagonal close-packing configuration. Our experimental data obtained for Li^+-incorporated MnO_2 agrees with the results of Chen and Wittingham [12]. It appears that Li^+ or Na^+ ions are easily removed from the structure through ion exchange with Li^+ ions in the electrolyte, followed by manganese migration into the interlayer space, which causes a rapid capacity decay. On the other hand, the ion-exchange reaction between Mg^{2+} in the structure and Li^+ in the electrolyte takes place at slower rate probably due to the valence difference. Thus, Mg^{2+} ions remain stable in the interlayer region, resulting as shown in Fig. 7 in improved capacity retention of $Mg_{0.17}MnO_2{\cdot}H_2O$. Analysis of the structural changes of $Mg_{0.17}MnO_2{\cdot}H_2O$ during electrochemical cycling is in progress in our laboratory.

4. Conclusion

The manganese oxide film electrodes incorporated with Li^+, Na^+, or Mg^{2+} ions were synthesized by a one-step electrochemical deposition from an aqueous $MnSO_4$ solution in the

presence of a perchlorate salt of the cation. The XRD analysis indicated that the electrodeposited oxide films have a birnessite-type layered structure with a rhombohedral symmetry. The d_{001} value was determined to be 0.72 nm, indicating the presence of water molecules in the interlayer space. The galvanostatic charge–discharge experiments in 1 M $LiPF_6$-DME/PC solution demonstrated that the Mg^{2+}-intercalated MnO_2 electrode exhibits an initial discharge of 140 mAh g^{-1} and shows an improved capacity retention when compared with Li^+- or Na^+-intercalated MnO_2 electrodes. Although some improvements are still necessary to mitigate a capacity fade, this study demonstrates that the electrodeposition can be used as an effective technique to prepare birnessite-type layered manganese oxides for rechargeable lithium batteries.

References

[1] M.S. Whittingham, Chem. Rev. 104 (2004) 4271–4301.
[2] B. Ammundsen, J. Paulsen, Adv. Mater. 13 (2001) 943–956.
[3] F. Capitaine, P. Gravereau, C. Delmas, Solid State Ionics 89 (1996) 197–202.
[4] A.R. Armstrong, P.G. Bruce, Nature 381 (1996) 499–500.
[5] G. Vitins, K. West, J. Electrochem. Soc. 144 (1997) 2587–2592.
[6] S. Ching, D.J. Petrovay, M.L. Jorgensen, S.L. Suib, Inorg. Chem. 36 (1997) 883–890.
[7] J.W. Long, L.R. Qadir, R.M. Stroud, D.R. Rolison, J. Phys. Chem. B 105 (2001) 8712–8717.
[8] S. Franger, S. Bach, J. Farcy, J.-P. Pereira-Ramos, N. Baffier, J. Power Sources 109 (2002) 262–275.
[9] S. Komaba, N. Kumagai, S. Chiba, Electrochim. Acta 46 (2000) 31–37.
[10] R. Chen, P. Zavalij, M.S. Whittingham, Chem. Mater. 8 (1996) 1275–1280.
[11] R. Chen, T. Chirayil, P. Zavalij, M.S. Whittingham, Solid State Ionics 86–88 (1996) 1–7.
[12] R. Chen, M.S. Whittingham, J. Electrochem. Soc. 144 (1997) L64–L67.
[13] M. Tabuchi, K. Ado, H. Kobayashi, H. Kageyama, C. Masquelier, A. Kondo, R. Kanno, J. Electrochem. Soc. 145 (1998) L49–L52.
[14] M. Nakayama, S. Konishi, A. Tanaka, K. Ogura, Chem. Lett. 33 (2004) 670–671.
[15] M. Nakayama, M. Fukuda, S. Konishi, T. Tonosaki, J. Mater. Res. 21 (2006) 3152–3160.
[16] M. Nakayama, H. Tagashira, S. Konishi, K. Ogura, Inorg. Chem. 43 (2004) 8215–8217.
[17] G.Z. Sauerbrey, Z. Phys. 155 (1959) 206.